

Stability of the Rydberg H₃O Radical

Jong Keun Park

Department of Chemistry and Central Laboratory, Pusan National University, Pusan 609-735, Korea

Received March 10, 1999

Proton and charge transfers in water solvent have been an issue in the quantum dynamics and energetics of (H₂O)_n clusters.¹⁻¹⁷ Although the structure and solvent effect of hydrated and neutral water clusters in chemical and biological processes have been extensively investigated with the theoretical¹⁻¹¹ and experimental¹²⁻¹⁷ methods, the Rydberg (H₃O⁺)(e⁻)_{3s} radical has not been studied until now. The Rydberg (H₃O⁺)(e⁻)_{3s} radical can be formed in water clusters like the Rydberg (NH₄⁺)(e⁻)_{3s} radical. In the Rydberg (NH₄⁺)(e⁻)_{3s} radical,^{18,19} the stability and electronic structure of NH₄ depend greatly on the avoided curve crossing between the dissociative state of (NH₄⁺)(e⁻)_{3s} and the repulsive state emerging from (NH₃ + H). In ammonia clusters, NH₄ has been known to be stabilized by the complexation with ammonia species. The lifetime of the NH₄ radical in cluster was measured to be 13 pico second.¹⁹

In this work, we studied state-to-state correlation curves of the ground and excited states for H₃O dissociating into (H₂O + H). For the dissociation reaction, the molecular orbitals and geometric structures at each internuclear distance were optimized using the restricted open-shell Hartree-Fock method (ROHF), keeping C_{2v} symmetry. And the molecular orbitals and optimized structures were used as input for subsequent the singly and doubly excited configuration interaction (SDCI) calculations. That is, the molecular orbitals for a configuration interaction (CI) are determined with the ROHF's results. The singly and doubly excited configuration interaction (SDCI) calculation is used with the GAMESS package. By changing the internuclear distance, the entire procedure was repeated from H₃O to (H₂O + H). The internuclear distances [R_(OH)] range from 0.80 to 10.0 Å. The SDCIs for H₂O, H₃O⁺, and H₃O are also performed separately. The geometric structures of the ground states of H₂O, H₃O⁺, and H₃O are also optimized with the second-order Møller-Plesset (MP2) and coupled cluster with both single and double substitution [CCSD(T)] levels using GAUSSIAN 94. The basis sets chosen are the triple zeta basis on O (5311111/32111)²⁰ and H(511).²¹ Two extra d type polarization functions are added to oxygen (α_d = 2.22, 0.874)²² and one extra p type function is added to hydrogen (α_p = 0.990495).²³ The diffuse Rydberg basis functions (α_s = 0.08, 0.032; α_p = 0.051, 0.02; α_d = 0.345, 0.143)²² are further augmented on oxygen to describe the Rydberg states of H₂O and H₃O.

The geometric parameters and the relative energies of H₃O dissociating into (H₂O + H) are listed in Table 1 together with the ionization and excitation energies of H₂O and H₃O. There are no previous experimental and theoretical results on H₃O to compare with our results. Since the ground state of H₃O has an electron in a Rydberg 3s orbital, H₃O itself is

often called the Rydberg radical and H₃O is a semi-ionic structure described as (H₃O⁺)(e⁻)_{3s}. Therefore, in the ground geometric structure of H₃O, the equilibrium internuclear distance of R_{(OH)eq} ≈ 1.02 Å is longer than that [R_{(OH)eq} ≈ 0.962 Å] of H₂O. The bond length [R_{(OH)TS}] at the transition state is ≈ 1.21 Å, that is, the bond breaking takes place near the equilibrium geometry of H₃O. The energy barrier heights from the transition state to H₃O and (H₂O + H) are ≈ 0.11 and 0.93 eV, respectively. The energy gap between H₃O and (H₂O + H) is ≈ 0.82 eV. Because the ground potential of H₃O has an energy barrier of ≈ 0.11 eV along the OH bond rupture, H₃O is very unstable. Because of the weak interaction between the nucleus and a Rydberg electron, the ionization and excitation energies of H₃O are relatively low.

Potential energy curves for the ground and low lying excited states of H₃O dissociating into (H₂O + H) are drawn in Figure 1. They are labeled as ¹A₁, ²A₁, ³A₁, ¹B₁, and ²B₁, respectively. The potential energy of (H₂O + H) is set equal to zero. To represent the avoided curve crossing clearly, the broken lines indicate estimated diabatic potential energy curves and these were drawn by hands. The ground ²A₁ state of H₃O correlates with an antibonding orbital emerging from the [H₂O(¹A₁) + H(²S)] asymptote. This

Table 1. Geometric parameters and relative energies (eV) for the ground ²A₁ state along the H₃O radical dissociating into (H₂O + H). Ionization and excitation energies (eV) of H₃O and H₂O

	HF	SECI	SDCI	MP2 ^a	CCSD(T) ^a	MP2 ^b	exp ^c
R _{(OH)eq} ^d	0.984	0.984	1.018	1.021	1.020		
(∠ HOH) _{eq} ^e	107.6	106.3	106.0	105.7	105.9		
R(OH) _{TS} ^d	1.174	1.122	1.213	1.215	1.210		
ΔE _(H₃O-TS)	0.19	0.13	0.12	0.11	0.11		
ΔE _[TS-(H₂O+H)]	1.45	1.07	0.97	1.01	0.93		
ΔE _[H₃O-(H₂O+H)]	-1.27	-0.94	-0.86	-0.90	-0.82		
H₃O							
I.E. ^f	4.73	4.95	5.30	5.32	5.34		
ΔE _{(3s-3p); ²A₁, ²B₁}		2.09	2.05				
ΔE _{(3s-4s); ²A₁}		2.72	2.80				
ΔE _{(3s-3d); ²A₁}		2.99	3.04				
H₂O							
I.E. ^g	11.06	12.50	12.54	12.56	12.52	12.63	12.6 ^{c,i}
P.A. ^h	7.60	7.44	7.32	7.39	7.30	7.08, 7.45 ^j , 7.18 ^j	7.79 ^k
ΔE _{(1b₁-3s); ¹A₁}		6.90	6.51				6.67
ΔE _{(1b₁-3p_{x,y}); ¹A₁}		10.27	10.21				10.17

^aMP2 energies were obtained with GAUSSIAN 94. ^bRef. 10. ^cRef. 15. ^dUnit of internuclear distance is angstrom. ^eUnit of angle is degree. ^fIonization energy of H₃O. ^gIonization energy of H₂O. ^hProton affinity of H₂O. ⁱRef. 13. ^jRef. 9. ^kRef. 11.

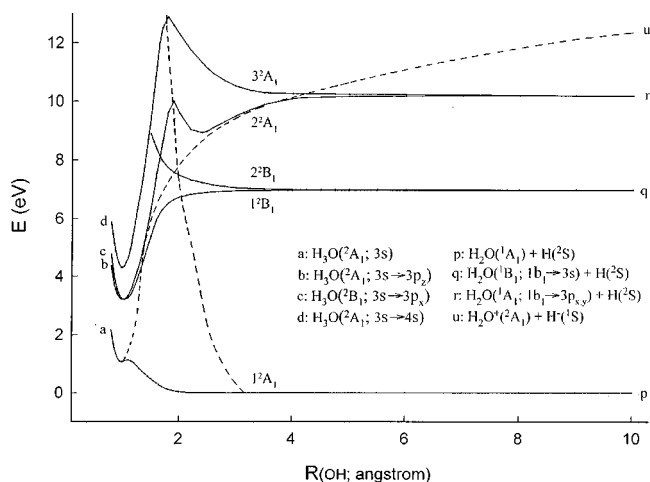


Figure 1. Potential energy curves for the ground and low lying excited states of the Rydberg H_3O radical dissociating into $(\text{H}_2\text{O} + \text{H})$.

curve is quasibound, which means that its equilibrium energy is higher than that of the dissociation asymptote of $(\text{H}_2\text{O} + \text{H})$. The potential curve has an energy barrier near the equilibrium geometry of H_3O . It is made by an avoided curve crossing between the dissociative diabatic state of the Rydberg $[(\text{H}_3\text{O}^+)(e^-)_{3s}]$ radical and the repulsive diabatic state emerging from an antibonding orbital of the $[\text{H}_2\text{O}(^1\text{A}_1) + \text{H}(^2\text{S})]$ asymptote. The barrier height and potential well are very low and shallow, respectively. The maximum position [$R_{(\text{OH})} \approx 1.21 \text{ \AA}$] of the transition state of the ground potential curve is located out of line of those [$R_{(\text{OH})} \approx 1.95 \text{ \AA}$] of the first and higher excited states.

In H_3O dissociating into $(\text{H}_2\text{O} + \text{H})$, the ground Rydberg H_3O radical diabatically dissociates into two kinds of asymptotes, that is, H_3O diabatically dissociates into the $[\text{H}_2\text{O}(^1\text{A}_1; 1b_1 \rightarrow 3p_{x,y}) + \text{H}(^2\text{S})]$ and $[(\text{H}_2\text{O}^+)^*(^2\text{A}_1) + \text{H}(^1\text{S})]$ asymptotes. In the second dissociation path, one electron jumps from the $1b_1$ orbital of H_2O to the $1s$ orbital of H . The ion pair has strongly attractive ionic character as the ions approach each other. Therefore, by avoided curve crossing between two dissociative diabatic states of $[(\text{H}_3\text{O}^+)(e^-)_{3s}]$ and the repulsive diabatic state emerging from $[\text{H}_2\text{O}(^1\text{A}_1) + \text{H}(^2\text{S})]$, the potential well and barrier height should be very deep and high, respectively. But, since the energy gap between the $[\text{H}_2\text{O}(^1\text{A}_1) + \text{H}(^2\text{S})]$ and $[\text{H}_2\text{O}(\tilde{D}^1\text{A}_1) + \text{H}(^2\text{S})]$ asymptotes is large, the potential energy barrier of the ground $^2\text{A}_1$ state is shifted to the equilibrium geometry of H_3O . The barrier height of the curve is found to be very low.

The dominant configuration for the ground $^2\text{A}_1$ state is $[\text{core}]2a_1^2 1b_2^2 3a_1^2 1b_1^2 4a_1$ at the H_3O structure and $[\text{core}]2a_1^2 1b_2^2 3a_1^2 1b_1^2 (4a_1)_\text{H}$ at large distance [$R_{(\text{OH})} = 10.0 \text{ \AA}$]. $2a_1^2 1b_2^2 3a_1^2 1b_1^2$ is an electronic configuration of H_3O^+ . $4a_1$ indicates an electron of the Rydberg $3s$ orbital having a H_3O^+ structure as a core. Therefore, the electronic structure of H_3O appears to be $[(\text{H}_3\text{O}^+)(e^-)_{3s}]$. H_3O is a semi-ionic state. Along OH bond rupture, the $4a_1$ orbital is non-bonding, *i.e.*, a character of $1s$ of H . $4a_1$ indicates one electron in the $1s$ orbital of H .

Generally, the ground-to-Rydberg transition energies are found to be higher than 5 eV-6 eV. But, in H_3O the Rydberg excitation energy is found to be low, that is, the excitation energy ($3s \rightarrow 3p$)_{Rydberg} is $\approx 2.05 \text{ eV}$. While, in H_2O the excitation energy ($1b_1 \rightarrow 3p_{x,y}$) is $\approx 10.21 \text{ eV}$. In the correlation curve, if the potential energy barriers of the ground and excited states are determined by the avoided curve crossings, the barrier height should be high and the maximum position should be located at the middle place between H_3O and $(\text{H}_2\text{O} + \text{H})$. But, in our ground potential curve of the dissociation, the potential energy barrier of $\approx 0.11 \text{ eV}$ is located near the equilibrium geometry of H_3O . In the avoided curve crossing between the attractive diabatic states emerging from $[\text{H}_2\text{O}(^2\text{A}_1) + \text{H}(^2\text{S})]$ and $[(\text{H}_2\text{O}^+)^*(^2\text{A}_1) + \text{H}(^1\text{S})]$ and the repulsive state from an antibonding interaction of $[\text{H}_2\text{O}(^1\text{A}_1) + \text{H}(^2\text{S})]$, the energy gap between two asymptotes plays an important role in the ground correlation curve. As a result, the position of the potential barrier is shifted to the equilibrium geometry of H_3O . That is, the maximum position of potential barrier of the ground state formed by the avoided curve crossing is located out of line of those of the excited potential energy curves. And the barrier height is found to be very low. Because of the low barrier, the existence of the Rydberg H_3O radical has not been observed experimentally.

In the excited $^2\text{A}_1$ state, the curve crossing between the dissociative diabatic excited states of $(\text{H}_3\text{O}^+)(e^-)_{\text{Rydberg}}$ and the repulsive diabatic states from the antibonding interaction of $[\text{H}_2\text{O}(^1\text{A}_1) + \text{H}(^2\text{S})]$ are found around $R_{(\text{OH})} \approx 1.5 \text{ \AA}$ and 4.0 \AA . In the excited $^2\text{B}_1$ ($3s \rightarrow 3p_x$) state of H_3O , the state correlates with a bonding interaction of the $[\text{H}_2\text{O}(^1\text{B}_1; 1b_1 \rightarrow 3s) + \text{H}(^2\text{S})]$ asymptote. An antibonding interaction emerging from $[\text{H}_2\text{O}(^1\text{B}_1; 1b_1 \rightarrow 3s) + \text{H}(^2\text{S})]$ is found to be repulsive. By the avoided curve crossings between the attractive diabatic state emerging from the electrostatic attraction of $[(\text{H}_2\text{O}^+)^*(^2\text{B}_1) + \text{H}(^1\text{S})]$ and the other states with the same symmetry, the potential energy curves of the ground and excited states for the dissociation of H_3O into $(\text{H}_2\text{O} + \text{H})$ show an irregular shape. Our state-to-state correlation diagram gives detailed information of the crossing positions and barrier heights for H_3O dissociating into $(\text{H}_2\text{O} + \text{H})$.

Acknowledgment. The author thanks Prof. Sun and Mr. Do-Hoon Kim for their invaluable help.

References

- Guissani, Y.; Guillot, B.; Bratos, S. *J. Chem. Phys.* **1988**, *88*, 5850.
- Wei, D.; Salahub, D. R. *J. Chem. Phys.* **1994**, *101*, 7633.
- Tuckerman, M.; Laasonen, K.; Sprik, M.; Parrinello, M. *J. Chem. Phys.* **1995**, *103*, 150.
- Lobaugh, J.; Voth, G. A. *J. Chem. Phys.* **1996**, *104*, 2056.
- Vuilleumier, R.; Borgis, D. *Chem. Phys. Lett.* **1998**, *284*, 77.
- Newton, M. L. *J. Chem. Phys.* **1977**, *67*, 5535.
- Botschwina, P. *J. Chem. Phys.* **1986**, *84*, 6523.
- Peterson, K. A.; Xantheas, S. S.; Dixon, D. A.; Dunning, J. H. *J. Chem. Phys.* **1998**, *108*, 1000.

- Jr., T. H. *J. Phys. Chem.* **1998**, *102*, 2449.
9. Del Bene, J. E.; Mettee, H. D.; Frisch, M. J.; Luke, B. T.; Pople, J. A. *J. Phys. Chem.* **1983**, *87*, 3279.
10. Curtiss, L. A.; Raghavachari, K.; Trucks, G. W.; Pople, J. A. *J. Phys. Chem.* **1991**, *94*, 7221.
11. Bueker, H. H.; Uggerud, E. *J. Phys. Chem.* **1995**, *99*, 5945.
12. Honma, K.; Sunderlin, L. S.; Armentrout, P. B. *J. Chem. Phys.* **1993**, *99*, 1623.
13. Ng, C. Y.; Trevor, D. J.; Tiedemann, P. W.; Ceyer, S. T.; Kronebusch, P. L.; Mahan, B. H.; Lee, Y. T. *J. Phys. Chem.* **1977**, *67*, 4235.
14. Nagashima, U.; Shinohara, H.; Nishi, N.; Tanaka, H. *J. Chem. Phys.* **1986**, *84*, 209.
15. Herzberg, G. *Molecular Spectra and Molecular Structure. Electronic Spectra and Electronic Structure of Polyatomic Molecules*, Vol. III; Van Nostrand, New York, 1966.
16. Liu, D.-J.; Oka, T.; Sears, T. J. *J. Chem. Phys.* **1986**, *84*, 1312.
17. Yeh, L. I.; Okumura, M.; Myers, J. D.; Price, J. M.; Lee, Y. T. *J. Chem. Phys.* **1989**, *91*, 7319.
18. (a) Park, J. K. *J. Chem. Phys.* **1997**, *107*, 6795. (b) Park, J. K. *J. Chem. Phys.* **1998**, *109*, 9753.
19. (a) Fuke, K.; Takasu, R. *Bull. Chem. Soc. Jpn.* **1995**, *68*, 3309. (b) Fuke, K.; Takasu, R.; Misaizu, F. *Chem. Phys. Lett.* **1994**, *229*, 597.
20. Duijneveldt, F. B. *IBM Research Report NO. RJ* **1971**, 945.
21. Hasimoto, K.; Osamura, Y. *J. Chem. Phys.* **1991**, *95*, 1121.
22. Partridge, H.; Bauschlicher, Jr. C. W.; Langhoff, S. R. *Theor. Chim. Acta* **1990**, *77*, 323.
23. Huzinaga, S.; Andzelm, J.; Klobukowski, M.; Radzio-Andzelm, E.; Sakai, Y.; Tatewaki, H. *Physical Science Data: Gaussian Basis Sets for Molecular Calculations*, Vol. 16; Elsevier: Amsterdam, 1984.
-